IET Control Theory & Applications

Research Article

IET Journals
The Institution of Engineering and Technology

Regular quantisation with hysteresis: a new sampling strategy for event-based PID control systems

ISSN 1751-8644
Received on 30th January 2020
Revised 26th May 2020
Accepted on 28th July 2020
doi: 10.1049/iet-cta.2020.0128
www.ietdl.org

Oscar Miguel-Escrig[1] ✉, *Julio-Ariel Romero-Pérez*[1]

[1]*Department of System Engineering and Design, Universitat Jaume I, 12071 Av. Vicent Sos Baynat, Castellón, Spain*

✉ *E-mail: omiguel@uji.es*

Abstract: In this study, a new sampling strategy for networked control systems, called regular quantification with hysteresis (RQH), is proposed. This alternative presents some benefits with respect to symmetric-send-on-delta sampling, which is one of the most used strategies in the event-based proportional–integral–derivative (PID) control loops. The behaviour of the RQH is defined by two parameters, the signal quantification and hysteresis, whose effect on the overall system performance is studied and guidelines about its choice are given in terms of noise measurement and steady-state error. The limit cycle oscillations that could be induced by this sampling strategy are studied and new robustness measures to avoid them are proposed based on the describing function approach. The suitability of some tuning rules for continuous PI when applied to control systems with a RQH sampling is evaluated using the proposed measures. The results show that these tuning rules can be applied under certain conditions.

1 Introduction

In recent years, several works have been published about event-based control (EBC) of continuous systems [1]. EBC allows to economise the data flow through the digital networks on networked control systems, reducing the data drop out in the form of packet losses and decreasing the delays introduced by the communication infrastructures. This is due to the fact that new data are only sent when significant changes are detected on the state of the system, instead of periodically as in the case of time-driven controllers. That is why EBC may be considered as one of the most promising control approaches in networked control systems, whose importance in modern factory automation has been recently recognised in [2]. An updated and extensive study about the main contributions to EBC during the last twenty years can be found in [3].

Among the control strategies adapted to the EBC paradigm, the PID algorithm has caught a special attention. It is undeniable that nowadays proportional–integral–derivative (PID) is used in most of the industrial control applications. Some data about the prevalence of PID in industry are given in [4] showing that >95% of the controllers are of this type. In the same line, a survey conducted among the industrial committee members' of the International Federation of Automatic Control published in [5] shows the dominant position of PID algorithms with respect to other advanced control strategies as MPC. Recently, the primordial role of PID in the context of Industry 4.0 has been highlighted in [6], as well as the necessity of introducing new features to adapt this well established control technology to this new paradigm, whose one of the most distinctive signs is the high connectivity between devices through wired and wireless communication networks. This fact, jointly with the dominance of PID in industry mentioned before, has encouraged the development of many researches about the event-based PID controllers during the last decades.

To the authors' knowledge, one of the firsts works about event-based PID (EBPID) was presented in [7]. In that paper, some issues were addressed related to the error in the calculation of the integral and derivative terms when the time between samples increases due to the irregular sampling. This problem was extensively treated some years later in the works of Durand and Marchand [8, 9] and Vasyutynskyy and Kabitzsch [10, 11]. Even though the goal in [7] was to use of the EBPID to reduce the use of CPU in embedded control systems without significantly affecting the closed-loop performance, the seminal ideas presented in that paper were afterwards extended to the case of EBPID in networked control systems.

As it was early shown [12], the sampling law determines the performance and behaviour of sampled control systems. In event-based control systems, the sampling strategies play an important role because they are in charge of generating the events for the execution of the controller's algorithm. Among these strategies, the ones based on the signal quantification have gained more and more relevance because of their ease of implementation. The most representative example is the send-on-delta (SOD) sampling, which is based on transmitting the value of a signal only when it crosses levels or thresholds of magnitude δ. The effectiveness of this strategy has been widely tested in terms of control performance and communication reduction [13, 14].

Inspired on SOD, in [15] a sampling strategy known as symmetric-send-on-delta (SSOD) was presented, which is characterised by including a hysteresis of the same value than the thresholds δ to the sampler. In the last years, several works have been presented about SSOD-based PI controllers, concerning both tuning procedures and application cases. In [16], the tuning of SSOD-based PI controllers for FOPTD systems was addressed and some rules were designed by minimising the 1% settling time of the closed-loop response. An application of SSOD event-based controllers to the inside air temperature control of the greenhouse production process was presented in [17]. In [18, 19], tuning methods for PI controllers with SSOD sampler have been developed based on new robustness margins for avoiding limit cycles that were obtained by applying the describing function (DF) technique and entail with the classical concepts of phase and gain margins. In [20], a unified design of a SSOD-based PID and Smith predictor for self-regulating and integral processes was investigated. A new system identification procedure based on the oscillations induced by SSOD sampling strategy was proposed in [21]. More recently, in [22] a procedure for tuning not only PI but also PID controllers with SSOD sampling for FOPTD systems was proposed. It is based on the definition of a new robustness measure to avoid limit cycle oscillations called the Tsypkin margin, presented in [23], which overcome the limitations of the DF approach. All these works reveal the interest in the SSOD-based controllers during the last decade.

Alternatively to the SSOD, another sampling strategy is the regular quantification (RQ), in which new data are sent whenever the value of the sampled signal is a multiple of the quantification

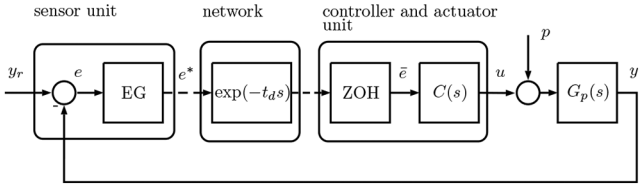

Fig. 1 *Control loop scheme for event-based PID controllers proposed in [15]*

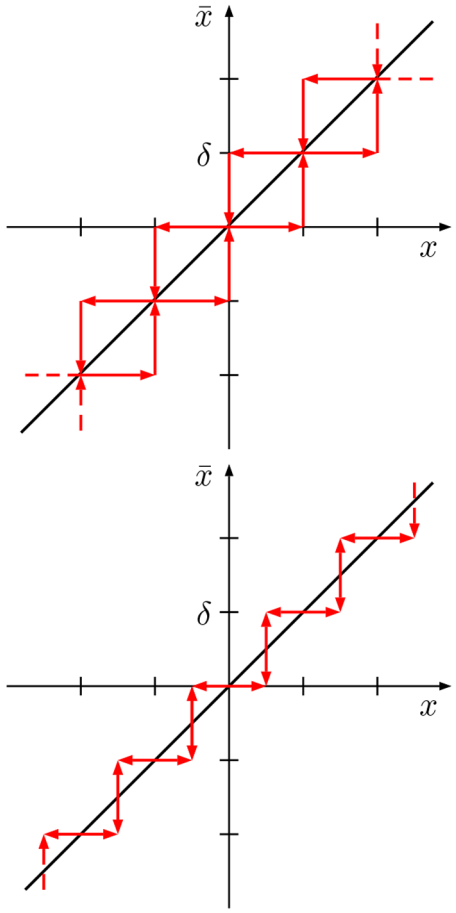

Fig. 2 *Input–output relation of SSOD (left) and RQ (right) sampling strategies*

threshold δ. A comparative study between SSOD and the RQ strategies has been presented in [24]. Due to the lack of hysteresis in the RQ sampler, bursts of events can appear due to the measurement noise, which is the main disadvantage of RQ with respect to SSOD. On the other hand, in RQ loops, the robustness against the limit cycle apparition is higher than in the SSOD loops for similar loop performances. These results suggest that the intermediate cases between RQ and SSOD sampling strategies could offer a better global behaviour because event generation due to noise can be avoided and robustness requirements may be not as restrictive as in the SSOD sampler.

The aforementioned researches in the field of EBPID show that, in general, conventional PID working under event-based sampling strategies hold its good performance-robustness trade-off while drastically reducing the data necessary to perform the control, and consequently the transmission through the digital network in networked systems is also decreased. The results presented in this paper delve into this approach by proposing new sampling strategies for event-based PI that improves the before mentioned drawbacks of the SSOD and RQ samplers.

The sampling law proposed here can be seen as a generalisation of the SSOD and RQ. The approach is based on selecting the hysteresis and the quantification threshold independently. This allows to disengage the immunity to noise from the reactivity of the controller to significant changes in the system. It is also proved that the new proposal can significantly reduce the number of generated events with respect to the SSOD strategy. The new sampler is studied in terms of robustness, developing quantitative measures to avoid the appearance of limit cycle oscillations.

Owing to in PID controllers the derivative action is very sensitivity to measurement noise, the PI control is the dominant form of the PID in use today [25]. As an example of the prevalence of PI among industrial control loops, the study presented in [26] reveals that >94% of controllers in power plants in Guangdong Province, China, is PI. Using the proposed robustness measures, the suitability of some well-known tuning methods used for designing continuous PI controllers is evaluated when applied to loops with PI controllers under the proposed sampling strategy. Concretely, the Ziegler-Nichols [27], Cohen–Coon [28] and AMIGO [29] methods are evaluated. These methods can be easily applied in industry because the controller parameters are straightforward calculated using very simple equations and data collected from the step response or the relay feedback experiments. Some previous studies developed by the authors have proved that AMIGO provides a proper tune for this kind of control scheme when SSOD sampling is used [22]. Among other results, the study in this paper demonstrates the validity of the AMIGO method to avoid the limit cycle oscillations when using PI with the proposed sampling law.

The paper is organised as follows. In Section 2, the problem statement is presented. Section 3 addresses the main characteristics and advantages of the proposed sampling strategy. Section 4 provides a study about the robustness against limit cycles that could be induced by this sampling approach. The study is based on the DF method and two new robustness margins are defined to avoid limit cycle oscillations. In Section 5, the aforementioned tuning methods are evaluated according to the proposed robustness margins considering a batch of processes. In Section 6, several simulation examples are presented. Finally, the conclusions about this work are drawn in Section 7.

2 Problem statement

Consider the networked control system shown in Fig. 1, where $C(s)$ and $G_p(s)$ are the controller and process transfer functions, respectively, the EG block represents the event generator, the ZOH block is a zero-order hold and $\exp(-t_d s)$ models the network's delay. Additionally, y_r is the reference signal, y is the controlled output and p is the perturbation input. It is assumed that the controller is located close to the actuator and that the event generator sends the measured signal e^* of the error e through the communication network and the ZOH block maintains in $\bar{e}$ the last sent value e^* until new data arrive. This control scheme was proposed in [15] considering that $C(s)$ is a PI controller and that the EG block is an SSOD sampler, thus, the authors named this architecture SSOD-PI. In a more general way, any controller and event generator can be used, therefore we will refer to this architecture as EG-$C(s)$.

As it has been mentioned before, two of the main sampling strategies used for event generation with fixed thresholds are the SSOD and RQ. The relation between a given input signal x and its respective output $\bar{x}$ for both sampling methods is shown in Fig. 2. The SSOD is characterised by sending new data whenever the sampled signal changes in a magnitude δ with respect to the last value sent, whereas the RQ sends new data whenever the signal crosses a value multiple of the quantification magnitude, δ, without any memory of the crossed thresholds.

As it was pointed in [24], with regard to the sampling of noisy signals, the SSOD can avoid the generation of extra events due to noise as long as its amplitude is lower than the hysteresis, whose value is equal to the threshold δ. Conversely, the RQ sampler is very sensitive to noise due to the lack of hysteresis, producing a high rate of events near to the crossing levels. On the other hand, regarding the robustness, the SSOD-$C(s)$ configuration propitiates the apparition of limit cycles, mainly due to the hysteresis, and thus, it requires more robust controllers than the RQ-$C(s)$, which admit faster controllers with lower robustness requirements. These

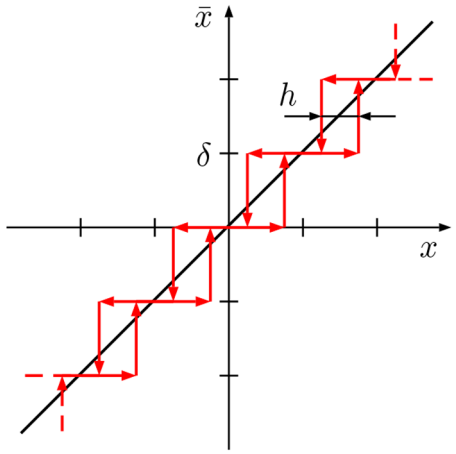

Fig. 3 *Input–output relation of the proposed sampling strategy with a hysteresis h*

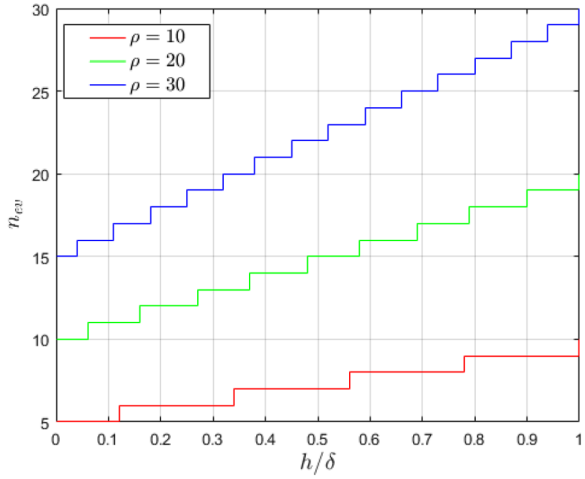

Fig. 4 *Influence of h/δ in the n_{ev} for different values of ρ*

negatives effects of SSOD and RQ in the control loop should be reduced in order to improve the overall performance of the control system. To this aim, a new sampling law is introduced in the next sections, whose properties are studied by defining new robustness measures to limit cycle.

It must be remarked that for processes with integrator the control system in Fig. 1 presents an oscillatory response, no matter the sampling strategy used in the block EG. This can be easily seen from the temporal response of the system: as long as the control action is not null, the process will keep integrating it and eventually the commutation thresholds will be reached, inducing the apparition of a limit cycles that are unavoidable for this kind of models. A control scheme based on SSOD sampling that prevents this kind of oscillations for integrating processes was proposed in [20]. Therefore, processes with integrator are out of the scope of this paper.

3 RQH sampling strategy

As SSOD and RQ are complementary with respect to their strengths and weaknesses, a new sampling strategy that gets an advantage of both is proposed. We have named this strategy as *Regular Quantisation with Hysteresis* (RQH), and its behaviour, i.e. the relation between an input signal $x(t)$ and its respective output $\bar{x}(t)$, is defined by (1) that includes two parameters, the quantisation level $\delta > 0$ and the hysteresis h that can be freely selected as long as $0 \leq h \leq \delta$. The input–output characteristic of the RQH sampler is presented in Fig. 3, where it can be easily seen that by fixing $h = 0$ or $h = \delta$ the RQ or SSOD samplers are obtained, respectively, thus, these sampling strategies are particular cases of RQH.

$$\bar{x}(t) = \begin{cases} (i+1)\delta \ \text{ if } \ x(t) \geq (i + \frac{1}{2} + \frac{h}{2\delta})\delta \text{ and } \bar{x}(t^-) = i\delta, \\ \qquad\qquad i \in \mathbb{Z} \\ (i-1)\delta \ \text{ if } \ x(t) \leq (i - \frac{1}{2} - \frac{h}{2\delta})\delta \text{ and } \bar{x}(t^-) = i\delta \\ i\delta \qquad \text{if } \ x(t) \in [(i - \frac{1}{2} - \frac{h}{2\delta})\delta, (i + \frac{1}{2} + \frac{h}{2\delta})\delta] \\ \qquad\qquad \text{and } \bar{x}(t^-) = i\delta \end{cases} \tag{1}$$

For intermediate values of h, the proposed method presents the characteristics of both SSOD and RQ. In general, the increment of h/δ reduces the event generation due to the noise for the same measured signal. More concretely, the inclusion of a hysteresis aims to eliminate the burst of events generated by the noise, which are eliminated whenever the amplitude of the noise lays within the hysteresis thresholds. Therefore, h must be selected slightly higher than the peak-to-peak amplitude of the noise.

The RQH sampling, as well as SSOD and RQ sampling, introduces a steady-state error on the system output of Fig. 1 because it exists a band around $e = 0$ in which the controller will receive a sampled error $\bar{e}$ equal to 0 but the value of e is between the commutation thresholds. This band should correspond to the values where there are not significant changes on the process output y. Equation (2) relates the admissible steady-state error in the controlled output (e_{ss}) with the parameters of RQH.

$$e_{ss} = \frac{1}{2}(\delta + h) \tag{2}$$

If h has been previously defined by considering the measured noise, then δ can be obtained directly from this expression to fulfil the e_{ss} requirement.

3.1 Event generation

One of the goals in the design of networked control systems is to reduce the data transmission through the network, which is directly related to the number of events generated by the sampler within the event-based control systems. With the proposed RQH sampling strategy, the number of events generated for a change of magnitude C in the input signal is

$$n_{ev} = \left\lfloor \frac{C - \frac{1}{2}(\delta + h)}{\delta} + 1 \right\rfloor \tag{3}$$

Combining expressions (2) and (3), we can find the relation between n_{ev}, h/δ, and C:

$$n_{ev} = \left\lfloor \frac{C - e_{ss}}{2e_{ss}}\left(1 + \frac{h}{\delta}\right) + 1 \right\rfloor \tag{4}$$

If the change C in the input signal is expressed in terms of the admissible steady-state error as $C = e_{ss}\rho$, then

$$n_{ev} = \left\lfloor \frac{\rho - 1}{2}\left(1 + \frac{h}{\delta}\right) + 1 \right\rfloor \tag{5}$$

Equation (5) describes the number of events generated by a RQH sampler with a given ratio h/δ when sampling an input signal with a change of magnitude $e_{ss}\rho$. Fig. 4 shows the relation between n_{ev} and h/δ for different values of ρ. It can be observed that the ratio h/δ significantly affects the amount of events for the same value of ρ. Concretely, the number of events obtained with an SSOD ($h/\delta = 1$) doubles the events generated by an RQ ($h/\delta = 0$). The RQH sampler presents intermediate values of n_{ev} between these extreme cases, reducing the amount of events as the h/δ is reduced. This influence in the number of events with respect to h/δ is stronger for higher values of ρ.

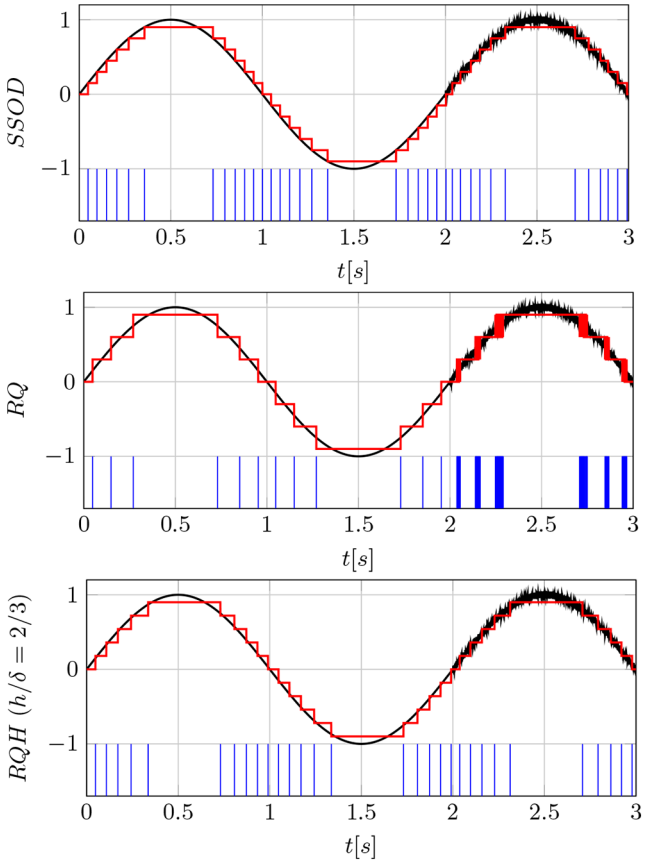

Fig. 5 *Sampled signal (red) resulting from a sinusoidal signal with and without noise (black) with the generated events (blue) using SSOD, RQ, and a RQH sampler with $h/\delta = 2/3$*

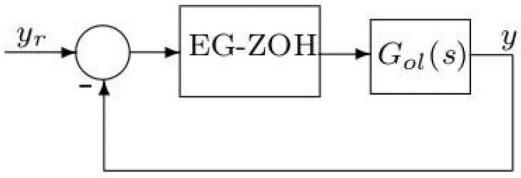

Fig. 6 *Block scheme equivalent to the one presented in Fig. 1*

With the aim of shedding further light on the advantages of the RQH sampler with respect to the SSOD and RQ strategies, let us introduce the following example.

Example 1: Consider three samplers (SSOD, RQ, and RQH) which should be configured to guarantee a maximum steady-state error $e_{ss} = 0.15$. In the case of SSOD and RQH, the samplers should also avoid the event generation due to a noise of 0.1 peak-to-peak amplitude. To fulfil these requirements, the parameter h of the RQH sampler must be selected slightly greater than the amplitude of the noise: $h = 0.12$. Then, δ can be calculated from (2) to meet the condition on e_{ss}: $\delta = 2e_{ss} - h = 0.18$. For the SSOD and RQ sampler, δ is determined by e_{ss}: for SSOD $\delta = e_{ss} = 0.15$ and for RQ $\delta = 2e_{ss} = 0.3$. In order to show the behaviour of the samplers, consider a sinusoidal input with unitary amplitude. During the first 2 s, the input to the sampler is a signal without noise, then the noise is added. The results produced by the samplers are shown in Fig. 5.

Firstly, it can be noted that the switching thresholds and the quantification produced by each sampler are different. This is due to the e_{ss} specification, which results in different δ for each sampler. For the RQ sampler, the number of events is significantly lower than that for the other two alternatives when a signal without noise is sampled. Nevertheless, for a noisy input, the RQ generates unnecessary events when the input is close to the switching thresholds. The SSOD sampler keeps quantifying the signal without being disturbed by the noise, but, as it has the lowest switching thresholds, if we only consider the sampling of the signal without noise, the number of events generated is the highest one among the three samplers. By using the RQH, no bursts of an event due to the noise are observed. Moreover, the number of samples is lower than in the case of the SSOD sampler, effectively reducing the data transmission through the network.

Using the RQH, sampling strategy has some important implications on the loop performance. As it is shown in the precedent example, the RQH sampler offers a reduction in the data transmission through the network with regard to RQ and SSOD sampling techniques. Nevertheless, regarding the control action bumps due to a change of magnitude δ in the sampler output $\delta_u = K_p\delta$, it is clear that by choosing the sampler parameters as in Example 1, these control action bumps will be greater for the RQH than for the SSOD sampling because the value of δ is greater for the first one.

Despite this prejudicial effect, choosing a RQH sampler has a big influence regarding the robustness requirements to design the controller $C(s)$ in order to avoid limit cycle oscillations induced by the sampler. This issue is studied in the next section.

4 Robustness to oscillation induced by RQH

The sampling strategy strongly influences the robustness against limit cycle oscillations induced by the sampler. This kind of robustness can be successfully characterised by using the DF technique, as proved in [19, 24]. To this aim, the block scheme presented in Fig. 1 can be rewritten as that in Fig. 6, where $G_{ol}(s) = C(s)G(s)$ is the open-loop transfer function, and $G(s) = G_p(s)e^{-t_d s}$ includes the plant model and the network delay. The EG-ZOH block samples the signal according to the RQH law and holds the last value sampled until the switching conditions are fulfilled, then, a new sample is taken and held again. Thus, it is clear that the combination of the sampling strategy block and the *ZOH* results in a non-linearity, and consequently it can be studied with the DF method.

It is well known that the condition for the existence of limit cycle in the system of Fig. 6 is given by

$$G_{ol}(j\omega) = -\frac{1}{\mathcal{N}}, \quad \forall\omega, \tag{6}$$

where $\mathcal{N}$ is the DF of the non-linearity. The graphical interpretation of (6) is that the system does not present limit cycle if the plots of $G_{ol}(j\omega)$ and $-\frac{1}{\mathcal{N}}$ do not intersect. The DF for the proposed RQH sampling strategy, including the parameters h and δ, is given by the following equation (see the Appendix of Section 10):

$$\mathcal{N}(A,h) = \frac{2\delta}{A\pi}\left[\sum_{k=1}^{m}\sqrt{1-\left(\frac{\delta}{A}\left(k+\frac{h}{2\delta}-\frac{1}{2}\right)\right)^2} + \sum_{k=m+1}^{2m}\sqrt{1-\left(\frac{\delta}{A}\left(2m-k-\frac{h}{2\delta}+\frac{1}{2}\right)\right)^2}\right] - j\frac{2hm\delta}{A^2\pi}, \tag{7}$$

where A is the amplitude of the sinusoidal oscillation and $m = \left\lfloor \frac{A}{\delta} - \frac{h}{2\delta} + \frac{1}{2} \right\rfloor$, i.e. the maximum number of levels crossed by the oscillation. From this expression, the SSOD and the RQ DFs can be obtained by replacing $h = \delta$ and $h = 0$, respectively. However, the most interesting cases are found in the range $h \in]0, \delta[$, where all the intermediate cases between SSOD and RQ appear.

Fig. 7 depicts the shapes of $-1/\mathcal{N}$ for different values of h/δ. The locus of $-1/\mathcal{N}$ are composed of several branches, one for each value of m. All the branches tend to fold and move towards the real-axis as h/δ decreases. The case in Fig. 7, where $h/\delta = 1$ represents the negative inverse of $\mathcal{N}$ for SSOD, whose study was addressed, together with the case of the RQ sampler, by the authors in [24], where some measures were defined to characterise their robustness against limit cycle oscillations. Nevertheless, to take

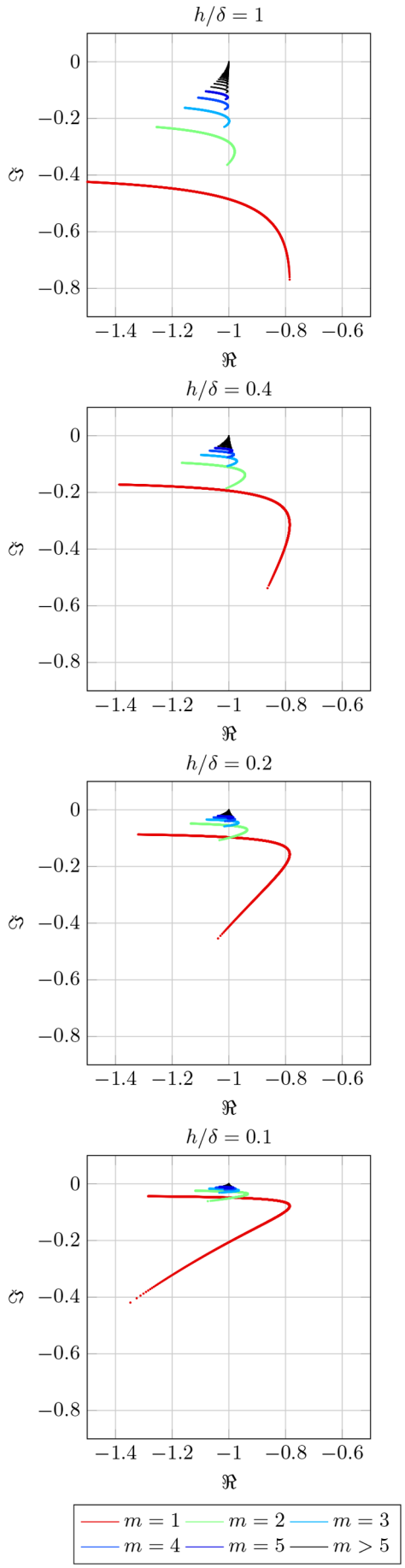

Fig. 7 *Shapes of $-1/\mathcal{N}$ for RQH samplers with different values of h/δ*

into account the intermediate cases between SSOD and RQ, presented in Fig. 7 when $h/\delta \neq 1$, new robustness measures must be defined.

Similar to the classical gain and phase margins, we have defined the gain margin to the non-linearity ($\gamma_{h/\delta}$) as the increment in the G_{ol} gain before reaching the intersection with $-1/\mathcal{N}$:

$$\gamma_{h/\delta} = \frac{\left|-\frac{1}{\mathcal{N}(A_\gamma)}\right|}{\left|G_{ol}(\mathrm{j}\omega_\gamma)\right|}, \tag{8}$$

where ω_γ and A_γ are the values of ω and A for which the quotient $\frac{\left|-\frac{1}{\mathcal{N}(A)}\right|}{|G_{\text{ol}}(\mathrm{j}\omega)|}$ is minimum while fulfilling the condition $\arg(G_{\text{ol}}(\mathrm{j}\omega)) = \arg\left(-\frac{1}{\mathcal{N}(A)}\right)$. This can be written in a compact form as

$$(\omega_\gamma, A_\gamma) = \arg\min_{(\omega, A)} \left(\frac{\left|-\frac{1}{\mathcal{N}(A)}\right|}{|G_{\text{ol}}(\mathrm{j}\omega)|} : \arg(G_{\text{ol}}(\mathrm{j}\omega)) = \arg\left(\frac{-1}{\mathcal{N}(A)}\right) \right). \tag{9}$$

On the other hand, the phase margin to the non-linearity ($\Phi_{h/\delta}$) is the minimum amount of phase required by G_{ol} to intersect the non-linearity while fulfilling the condition $\left|-\frac{1}{\mathcal{N}(A)}\right| = \left|G_{\text{ol}}(\mathrm{j}\omega)\right|$. That is

$$\Phi_{h/\delta} = \arg(G_{\text{ol}}(\mathrm{j}\omega_\Phi)) - \arg\left(-\frac{1}{\mathcal{N}(A_\Phi)}\right), \tag{10}$$

where ω_Φ and A_Φ are the values of ω and A for which the difference $\arg(G_{\text{ol}}(\mathrm{j}\omega)) - \arg\left(-\frac{1}{\mathcal{N}(A)}\right)$ is minimum while fulfilling the condition $\left|-\frac{1}{\mathcal{N}(A)}\right| = \left|G_{\text{ol}}(\mathrm{j}\omega)\right|$. This can be written in a compact form as

$$(\omega_\Phi, A_\Phi) = \arg\min_{(\omega, A)} \left(\arg(G_{\text{ol}}(\mathrm{j}\omega)) - \arg\left(-\frac{1}{\mathcal{N}(A)}\right) : \left|-\frac{1}{\mathcal{N}(A)}\right| = \left|G_{\text{ol}}(\mathrm{j}\omega)\right| \right). \tag{11}$$

It is important to note that, as proved in [19, 24] for the cases SSOD and RQ, for PI controllers tuned with reasonable values of gain and phase margins the shape of G_{ol} is such that the non-intersection with the branch corresponding to $m = 1$ guarantees no intersections with branches for $m > 1$, and consequently, no intersection between G_{ol} and $-1/\mathcal{N}$ takes place. Therefore, in most of practical cases, the limit cycles can be effectively eliminated by avoiding the intersection between G_{ol} and the branch of $-1/\mathcal{N}$ corresponding to $m = 1$, and the margins $\gamma_{h/\delta}$ and $\Phi_{h/\delta}$ are measured with respect to this branch.

Fig. 8 shows the margins $\gamma_{h/\delta}$ and $\Phi_{h/\delta}$ in the Nyquist and Nichols diagrams for a given system and a given value of h/δ. In this figure, only the branch $m = 1$ of $-1/\mathcal{N}$ has been represented. These robustness measures are easily visualised on Nichols chart because they are, similar to the traditional gain and phase margins, the vertical and horizontal minimum distances from the $G_{\text{ol}}(\mathrm{j}\omega)$ to the negative inverse of $\mathcal{N}$.

As postulated in [30], the condition for avoiding limit cycle oscillation results from a generalisation of the Nyquist stability criterion by considering the DF as a generalised gain. This generalisation states that the entire Nyquist curve of the open-loop transfer function must encircle anticlockwise the critical points $(-1/\mathcal{N}, 0)$ the number of times equal to the number of poles with the positive real part in G_{ol}. Therefore, if neither the plant $G_p(s)$ nor the controller $C(s)$ have poles with the positive real part, the Nyquist curve should not encircle the negative inverse of the DF for avoiding limit cycles. This fact allowed us to define the margins $\gamma_{h/\delta}$ and $\Phi_{h/\delta}$ to measure the distance between $-1/\mathcal{N}$ and G_{ol} when encircles are not required for the stability. According to that, these

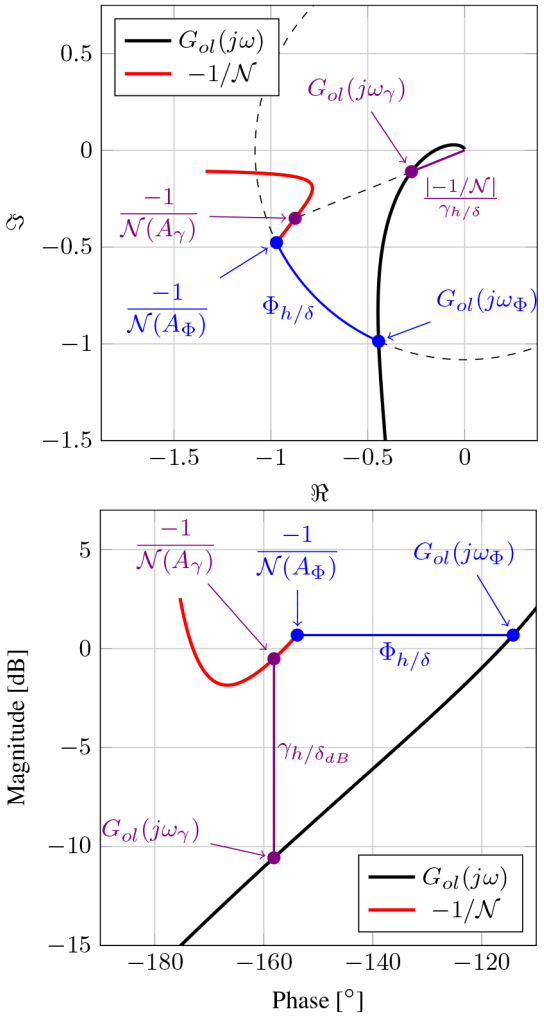

Fig. 8 *Gain and phase margins to the non-linearity* $(\gamma_{h/\delta}, \Phi_{h/\delta})$ *for a given open-loop transfer function* G_{ol} *in Nyquist and Nichols diagrams*

margins cannot be applied to plants whose poles have a positive real part.

The proposed margins guard the traces of $-1/\mathcal{N}$ against intersections with $G_{\text{ol}}(s)$ due to modelling errors or variations in the plant dynamics and network delay. If the open-loop transfer function for the nominal plant does not cross the boundary defined by $\gamma_{h/\delta}$ and $\Phi_{h/\delta}$, the system will remain without oscillations for a certain range of variation on the plant parameters. The magnitude of the admissible variations is strongly influenced by the structure of the plant model $G_p(s)$, so it has to be studied for each specific case. The robustness can be also affected by the variation on the network delay, which is always present in the control system under study. The effect of variation on this parameter is addressed next.

4.1 Network communication delay influence on the robustness margins

The effect of the delay introduced by the communication network on the robustness margins is considered by including the term $e^{-t_d s}$ in the open-loop transfer function. However, variations on t_d could degrade the robustness against limit cycle oscillations. To study the influence of this parameter on $\gamma_{h/\delta}$ and $\Phi_{h/\delta}$, consider a variation on t_d: $t'_d = t_d \pm \alpha$. Then the open-loop transfer function is

$$G'_{\text{ol}}(\text{j}\omega) = G_{\text{ol}}(\text{j}\omega)e^{\mp \text{j}\omega\alpha} \tag{12}$$

This equation can be expressed in terms of magnitude and phase as

$$\begin{cases} |G'_{\text{ol}}(\text{j}\omega)| = |G_{\text{ol}}(\text{j}\omega)| \\ \arg\{G'_{\text{ol}}(\text{j}\omega)\} = \arg\{G_{\text{ol}}(\text{j}\omega)\} \mp \omega\alpha \end{cases} \tag{13}$$

from which it can be seen that variations on the network delay correspond to horizontal displacements of $G_{\text{ol}}(\text{j}\omega)$ in the Nichols diagram. Concretely, the resulting open-loop transfer function will approach to the negative inverse of the DF traces as t'_d increases, worsening both $\gamma_{h/\delta}$ and $\Phi_{h/\delta}$. On the other hand, the reduction of t'_d improves both margins. Due to this effect, the higher value of admissible delays introduced by the network should be considered as t_d to avoid the degradation of the margins due to the variation on this parameter.

It must be remarked that, depending on the process dynamics defined by $G_p(s)$, the network delay can be neglected because of its minor influence on G_{ol}, and consequently on the robustness margins. In those cases, the delay term can be omitted from the open-loop transfer function.

5 Evaluation of classical tuning methods using the proposed margins

To illustrate the usefulness of the proposed margins we have applied them to study the robustness against limit cycle oscillations induced by PI controllers with transfer function

$$C(s) = K_p\left(1 + \frac{1}{T_i s}\right), \tag{14}$$

tuned with well known methods when the controllers are used under the RQH sampling strategy scheme as that in Fig. 1. The tuning methods selected for this study are Ziegler–Nichols [27], Cohen–Coon [28] and AMIGO [29]. PI controllers have been tuned for the batch of models presented below, which describe a wide range of behaviours that can be found in actual real systems. The dynamic responses of the models in the batch were approximated by first-order plus time delay (FOPTD) models to obtain the parameters of their respective controller. The robustness margins $\gamma_{h/\delta}$ and $\Phi_{h/\delta}$ have been calculated in all cases.

$$\begin{aligned}
G(s) &= \frac{e^{-s}}{(Ts+1)^2}, \\
T &= 0.01, 0.02, 0.05, 0.1, 0.2, 0.3, 0.5, 0.7, 1, \\
&\quad 1.3, 1.5, 2, 4, 6, 8, 10, 20, 50, 100, 200, 500, \\
G(s) &= \frac{1}{(s+1)(Ts+1)^2}, \\
T &= 0.05, 0.1, 0.2, 0.5, 2, 5, 10, \\
G(s) &= \frac{1}{(s+1)^n}, \\
n &= 3, 4, 5, 6, 7, 8, \\
G(s) &= \frac{1}{(s+1)(\alpha s+1)(\alpha^2 s+1)(\alpha^3 s+1)}, \\
\alpha &= 0.1, 0.2, 0.3, 0.4, 0.5, 0.6, 0.7, 0.8, 0.9, \\
G(s) &= \frac{Te^{-L_1 s}}{(T_1 s+1)(Ts+1)}, \\
T_1 + L_1 &= 1, \quad T = 1, 2, 5, 10, \\
L_1 &= 0.01, 0.02, 0.05, 0.1, 0.3, 0.5, 0.7, 0.9, 1, \\
G(s) &= \frac{1-\alpha s}{(s+1)^3}, \\
\alpha &= 0.1, 0.2, 0.3, 0.4, 0.5, 0.6, 0.7, 0.8, 0.9, 1, 1.1, \\
G(s) &= \frac{1}{(s+1)((sT)^2 + 1.4sT + 1)}, \\
T &= 0.1, 0.2, 0.3, 0.4, 0.5, 0.6, 0.7, 0.8, 0.9, 1.
\end{aligned} \tag{15}$$

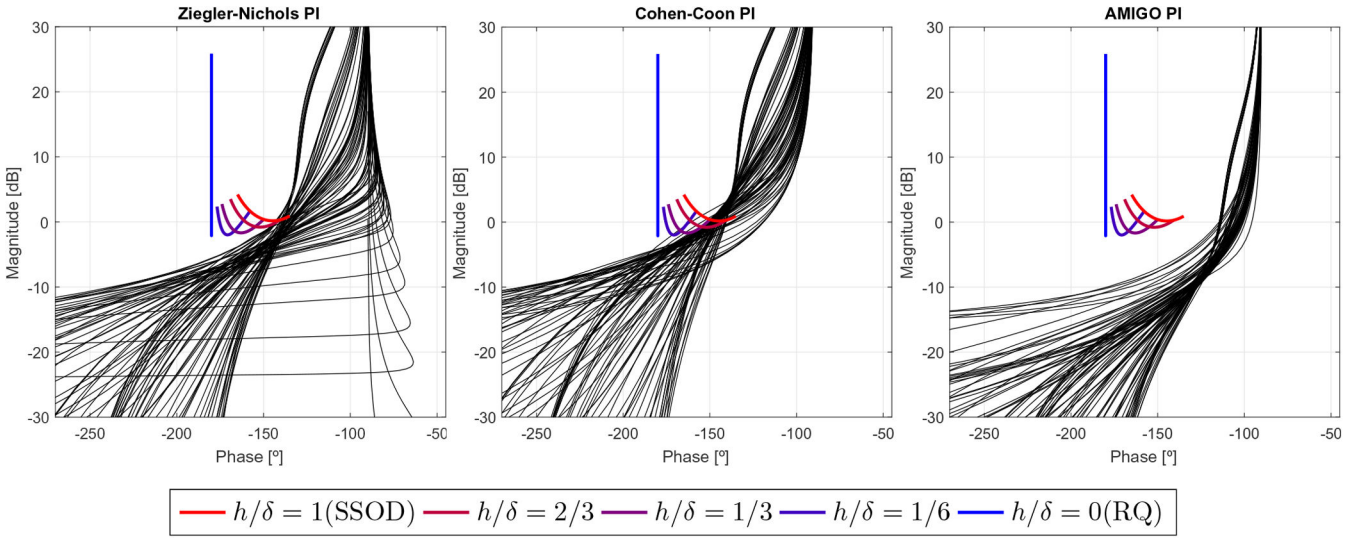

Fig. 9 *Nichols plots of the presented batch of processes with the specified controllers and the traces of $-1/\mathcal{N}$ for $m = 1$ with different values of h/δ*

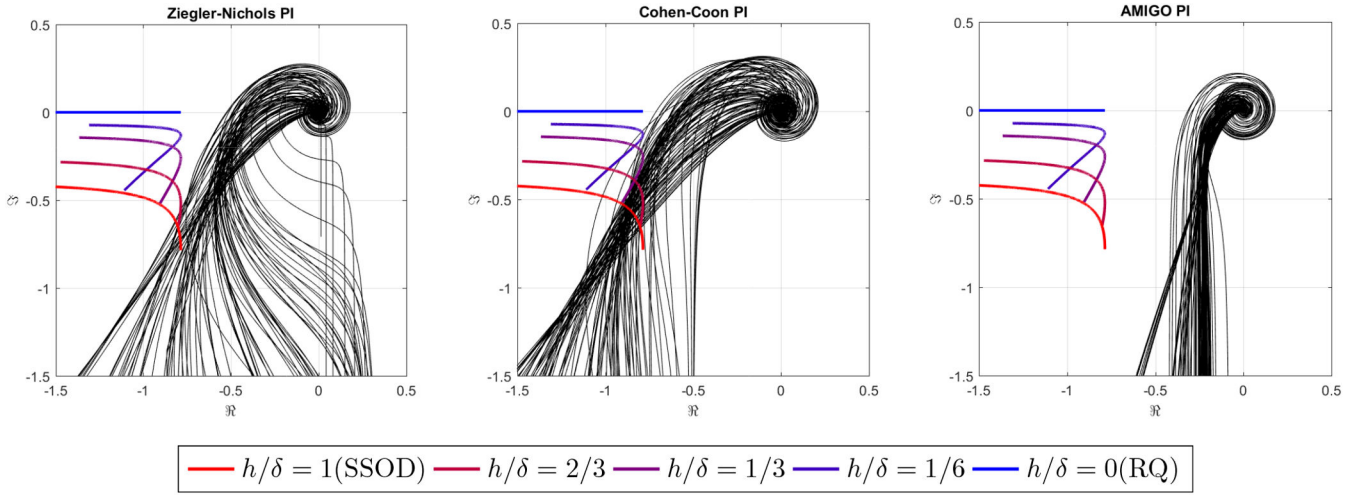

Fig. 10 *Nyquist plots of the presented batch of processes with the specified controllers and the traces of $-1/\mathcal{N}$ for $m = 1$ with different values of h/δ*

The open-loop transfer functions, $G_{\text{ol}}(s) = C(s)G(s)$, for all the designs are represented in the Nyquist and Nichols diagrams in Figs. 9 and 10, where the traces of $-1/\mathcal{N}$ for one level oscillations, $m = 1$, obtained for different ratios h/δ are also depicted. As commented before, the behaviour of these traces with the reduction of the ratio h/δ, in both Nyquist and Nichols diagrams, is to fold and tend to a straight line, horizontal on the real axis for the Nyquist diagram and vertical at -180° for the Nichols diagram, which corresponds to the RQ sampling.

From these figures, some conclusions can be drawn. Firstly, the Ziegler–Nichols and Cohen–Coon methods offer some controllers which make the open-loop transfer function to intersect with the negative inverse of the DF for some values of h/δ, and thus, these systems will oscillate when sampled with those strategies. Secondly, the AMIGO method offers controllers which avoid the intersection with $-1/\mathcal{N}$ and provide the higher values of $\gamma_{h/\delta}$ and $\Phi_{h/\delta}$, therefore, oscillations due to the RQH sampling will not take place, even for certain variations in the plant dynamic.

In view of these results, to assure that limit cycle oscillations will not take place, the proposed margins must be checked once the controller is tuned. To evaluate the robustness of a concrete design for particular variations in the plant model, the magnitude of changes in the plan dynamic must be expressed in terms of gain and phase variations of G_{ol}. If such variations are lower than the respective margins then the design in a robust enough. On the other hand, if as a consequence of changes in the dynamic behaviour of the plant, the margins $\gamma_{h/\delta}$ and $\Phi_{h/\delta}$ are surpassed, then instabilities will appear.

5.1 Influence of h/δ on the robustness margins

The margins $\gamma_{h/\delta}$ and $\Phi_{h/\delta}$ for different values of h/δ are shown in Figs. 11–13. The results corroborate the preliminary observations from Figs. 9 and 10. Firstly, it must be highlighted the good behaviour of PI controllers tuned with AMIGO rules, which have positive values of margins for all the batch processes and all ratios h/δ. It is also remarkable that for Ziegler–Nichols and Cohen–Coon methods, despite the fact of having reasonable values of classical phase and gain margins, which are also represented in the figure with dashed lines, for high values of h/δ some systems present negative values of $\gamma_{h/\delta}$ and $\Phi_{h/\delta}$, i.e. it exists an intersection between the open-loop transfer function and $-1/\mathcal{N}$. Particularly, critics are the results of the Cohen–Coon method whose margins are negative for most of the processes when h/δ is greater than 0.4.

Beyond the results obtained for each tuning method, the previous study reveals that the reduction of h/δ tends to increase both $\Phi_{h/\delta}$ and $\gamma_{h/\delta}$, being ultimately similar to the classical gain and phase margins when the RQ sampler is considered.

5.2 Influence of controller's parameters on the robustness margins

Concerning the influence of the controller parameters on the proposed margins, it is worth noting that both K_p and T_i modify the relative position of $G_{\text{ol}}(s)$ with regard to $-1/\mathcal{N}$. The effect of varying these parameters can be easily observed in the Nichols diagram because changes in K_p and T_i produce vertical and/or horizontal displacements on $G_{\text{ol}}(s)$.

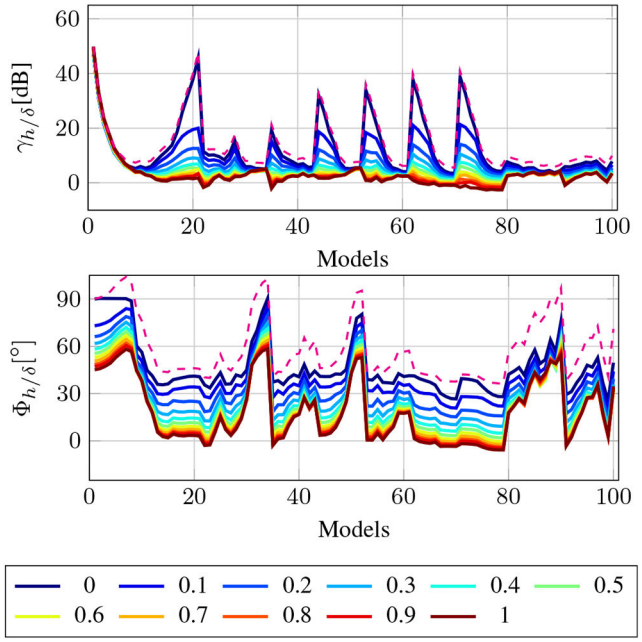

Fig. 11 *$\gamma_{h/\delta_{dB}}$ and $\Phi_{h/\delta}$ for several values of h/δ (solid coloured lines) and classical gain and phase margins (dashed magenta line) with Ziegler–Nichols tuning method*

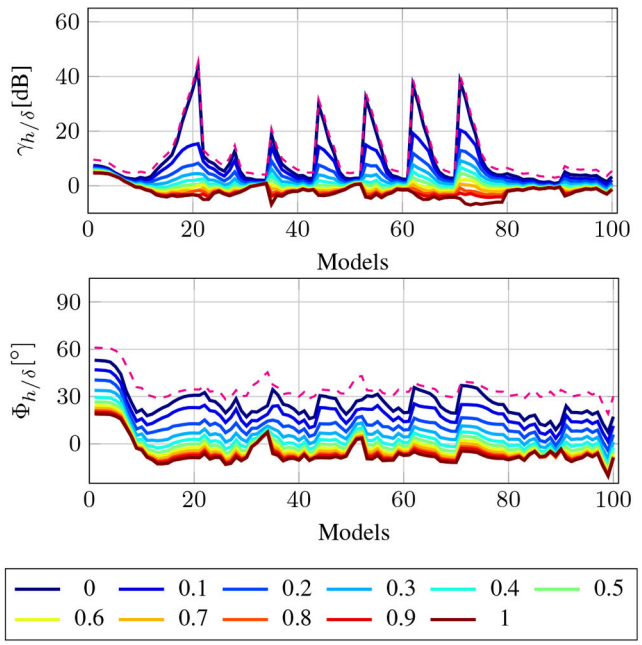

Fig. 12 *$\gamma_{h/\delta_{dB}}$ and $\Phi_{h/\delta}$ for several values of h/δ (solid coloured lines) and classical gain and phase margins (dashed magenta line) with Cohen–Coon tuning method*

The magnitude and phase expressions for a PI controller with transfer function in (14) are

$$|C(\mathrm{j}\omega)| = K_p\sqrt{1+\left(\frac{1}{\omega T_i}\right)^2} \tag{16}$$

$$\arg\{C(\mathrm{j}\omega)\} = \arctan\left(-\frac{1}{\omega T_i}\right) \tag{17}$$

From these expressions, it can be seen that the proportional gain produces a vertical displacement of $G_{\mathrm{ol}}(\mathrm{j}\omega)$ in the Nichols diagram. Concretely, the $G_{\mathrm{ol}}(\mathrm{j}\omega)$ moves down as K_p decreases, which, due to the shape of $G_{\mathrm{ol}}(\mathrm{j}\omega)$ depicted in Fig. 9, implies the improvement of both margins. On the other hand, the variation on the integral time produces both a vertical and horizontal displacement of $G_{\mathrm{ol}}(\mathrm{j}\omega)$. It can be seen that by increasing T_i a displacement downwards and to the right of $G_{\mathrm{ol}}(\mathrm{j}\omega)$ take place in the Nichols diagram, which implies an improvement of both margins.

According to these results, by detuning of the PI controllers (reducing K_p and/or increasing T_i) both margins can be raised. This behaviour of $\Phi_{h/\delta}$ and $\gamma_{h/\delta}$ respect to the controller parameters is qualitatively similar to that of the classical gain and phase margins, therefore, the detuning of the controller improves all the four margins at the expense of getting more slow closed-loop responses.

6 Simulation examples

In this section, the main issues related to the RQH sampler presented in this paper are illustrated through simulation examples.

Example 2: This example shows the influence of h/δ in the event generation. The number of generated events in $RQH-PI(s)$ loops strongly depends on the choice of the sampling parameters, i.e. hysteresis h and quantification δ. In Section 3.1, a study about the effect on the event generation of the ratio h/δ for samplers, which conduct to the same steady-state error was presented. In the following example, the influence of this choice is shown by comparing SSOD and RQH samplers.

Consider a process whose transfer function is described by

$$G_p(s) = \frac{e^{-0.3s}}{(s+1)(0.7s+1)}. \tag{18}$$

The network communication delay is tested to have a latency $t_d = 0.15$ s. Thus, the whole model to be considered for the tuning is described by

$$G(s) = \frac{e^{-0.45s}}{(s+1)(0.7s+1)}. \tag{19}$$

A PI controller has been tunned following Ziegler–Nichols tuning rules, obtaining $K_p = 1.52$ and $T_i = 2.58$. This controller does not make the open-loop transfer function intersect the traces of the inverse negative for any ratio h/δ, therefore, it avoids limit cycle oscillations induced by the sampler. This fact can be corroborated in Fig. 14, where the Nyquist diagram of $G_{\mathrm{ol}}(\mathrm{j}\omega)$ and the inverse negative of the DF for several ratios h/δ have been represented. As it can be seen, no intersection exist between $G_{\mathrm{ol}}(\mathrm{j}\omega)$ and the $-1/\mathcal{N}$ traces.

The measurement noise present in this loop is observed to have a peak-to-peak amplitude of 0.07 units and the admissible maximum steady-state error to provide a correct functioning is $e_{\mathrm{ss}} = 0.18$. With these requirements, following the guidelines in Section 3, the SSOD is chosen to have $\delta = 0.18$ to minimise the event generation and assuring the accomplishment of the specifications. With regard to the RQH sampler, to avoid event generation due to noise, the hysteresis is chosen to be $h = 0.08$, and, to fulfil the maximum e_{ss} criterion, $\delta = 0.28$.

Two experiments have been performed with the same process and controller but changing the sampler in the loop. The experiments consist in two unitary step changes at the reference input and a unitary step change in the disturbance input at different times. The results of the experiments can be seen in Figs. 15 and 16 for the SSOD and RQH samplers, respectively.

Regarding both figures, there are not remarkable differences which could make one sampler preferable over the other. In terms of the controlled output, both reach the steady-state regime in about 10 s. The unique difference resides in the number of events generated, which for the case of the SSOD is $n_{\mathrm{ev}} = 31$ and for the RQH is $n_{\mathrm{ev}} = 22$, reducing in a significant manner the number of generated events.

This example proves that by choosing a RQH sampler over an SSOD, the system performance is not significantly affected and the number of events generated is lower. Nevertheless, this event generation reduction implies that the control action bumps produced by a change of the magnitude δ at the input of the

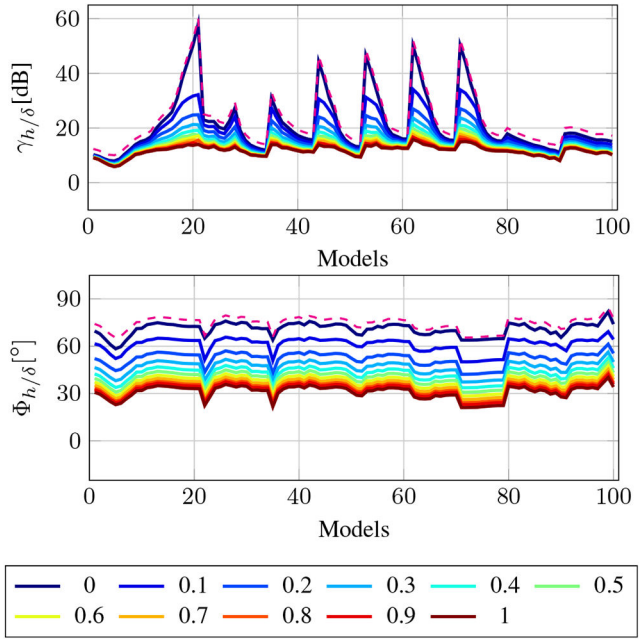

Fig. 13 *$\gamma_{h/\delta_{dB}}$ and $\Phi_{h/\delta}$ for several values of h/δ (solid coloured lines) and classical gain and phase margins (dashed magenta line) with AMIGO tuning method*

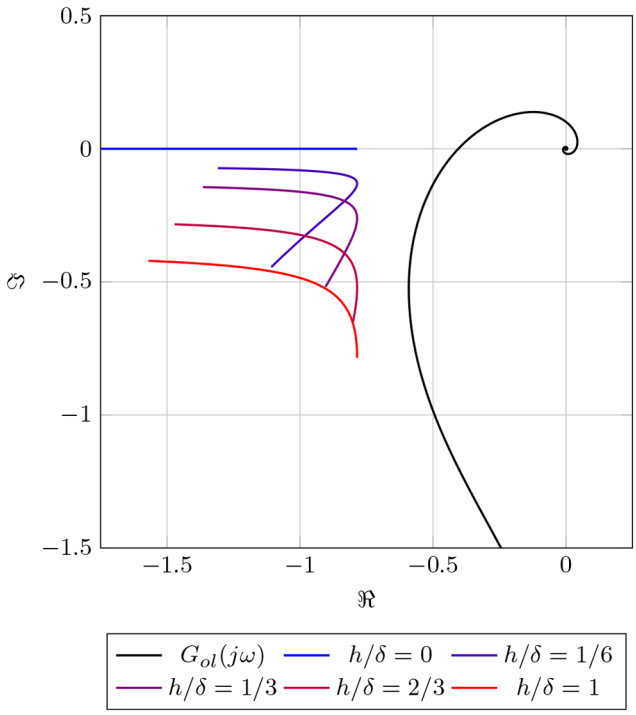

Fig. 14 *Nyquist diagram of $G_{ol}(j\omega)$ and the inverse negative of the DF corresponding to several samplers*

controller, $\delta_u = K_p\delta$, is higher for the RQH than for the SSOD. In this example, this control action bumps for the SSOD are $\delta_u = 0.274$ and for the RQH are $\delta_u = 0.426$.

Example 3: This example shows the usefulness of the DF approach on predicting the oscillation induced by the RQH sampler. As commented before, the ratio h/δ has a strong influence in the appearance of limit cycle because it changes significantly the shape of the inverse negative of the DF and, therefore, the robustness margins $\gamma_{h/\delta}$ and $\Phi_{h/\delta}$. In this example, the influence of the ratio h/δ on the robustness is highlighted.

Consider a process whose transfer function is described by

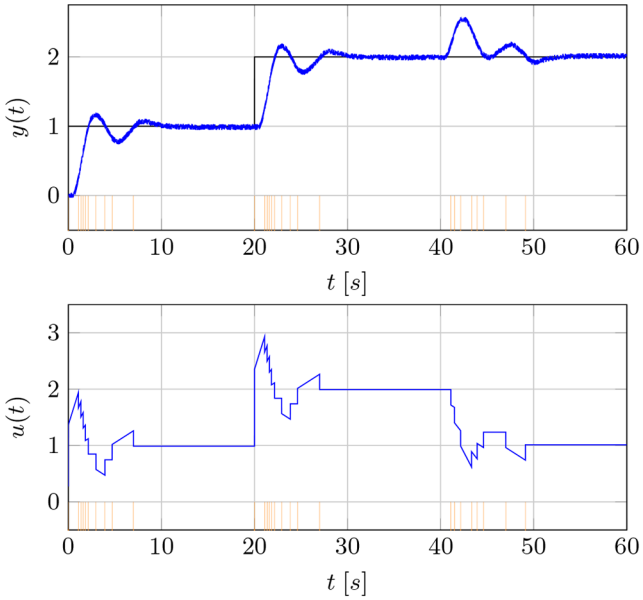

Fig. 15 *Controlled output y and control action u for the system containing an SSOD sampler, which results in a number of events generated $n_{ev} = 31$, marked in an orange*

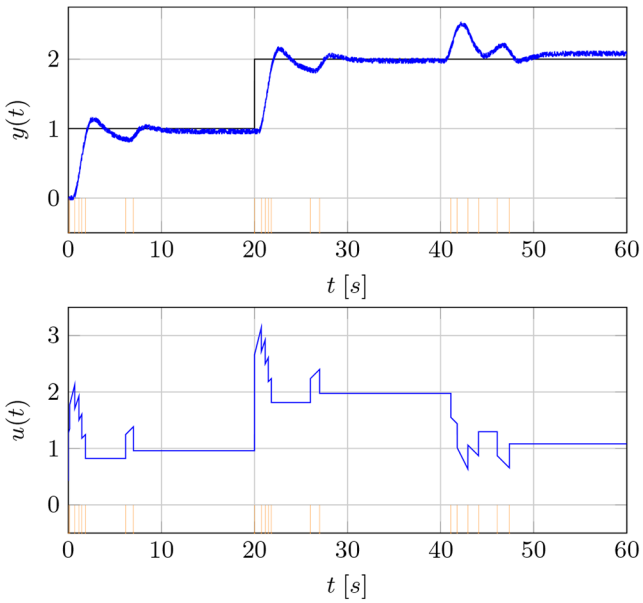

Fig. 16 *Controlled output y and control action u for the system containing a RQH sampler, which results in a number of events generated $n_{ev} = 22$, marked in an orange*

$$G_p(s) = \frac{1 - 0.1s}{(s+1)^3}. \tag{20}$$

The network communication delay is small enough with respect to the system dynamics, so it can be neglected. A PI controller has been tuned according to Cohen–Coon tuning rules, resulting in $K_p = 1.612$ and $T_i = 1.938$.

The measurement noise in the loop is observed to have a peak-to-peak amplitude of 0.03 units and the maximum admissible steady-state error is $e_{ss} = 0.1$. From this specifications, two RQH samplers will be designed and tested in the loop.

For the first sampler, consider a very conservative approach to avoid the event generation due to noise, in which the hysteresis will be selected to be twice the observed peak-to-peak amplitude $h = 0.06$ and the quantification δ is selected to meet the maximum admissible e_{ss}, $\delta = 0.14$, resulting in a sampler with ratio $h/\delta = 0.4286$.

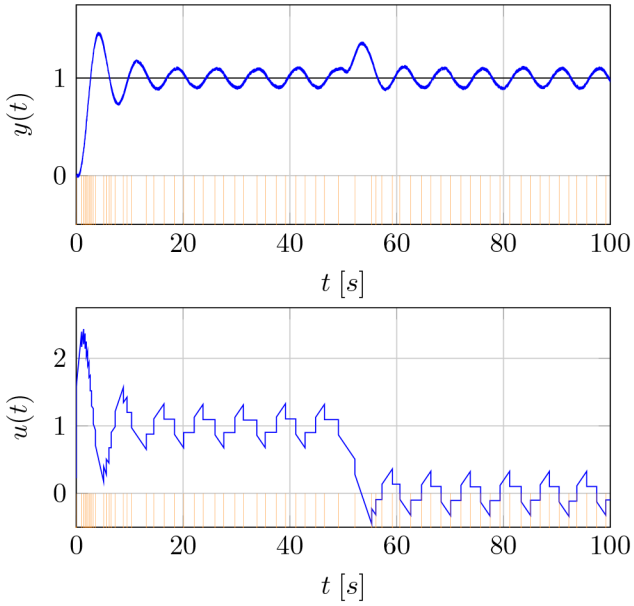

Fig. 17 *Controlled output y and control action u of a system with a RQH sampler with $h/\delta = 0.4286$ in the loop, which leads to an oscillatory response*

This system has been simulated and its temporal response to a unitary step change in the reference and disturbance inputs is presented in Fig. 17. As it can be seen, the resulting system response is oscillatory. This is justified in the previous section because, even if the classical gain $\gamma_{cp} = 6.5\,\text{dB}$ and phase $\Phi_{cg} = 30.37°$ margins for most of continuous applications provide enough robustness, the gain $\gamma_{h/\delta} = -0.4\,\text{dB}$ and phase $\Phi_{h/\delta} = -1.98°$ margins to the non-linearity obtained for the RQH with $h/\delta = 0.4286$ indicate the existence of an intersection between $G_{\text{ol}}(\text{j}\omega)$ and $-1/\mathcal{N}$ as corroborated in Fig. 18*a*, and therefore, it exists a limit cycle.

A more suitable RQH sampler is obtained by choosing the hysteresis $h = 0.04$ and δ to fulfil the e_{ss} requirement, $\delta = 0.16$, resulting in a ratio $h/\delta = 0.25$, which is lower than in the precedent case. With this new RQH sampler, the proposed robustness margins are recalculated, and the respective gain and phase margins, $\gamma_{h/\delta} = 1.15\,\text{dB}$ and $\Phi_{h/\delta} = 5.58°$, are obtained, which indicate that the oscillation condition is not satisfied, and then, limit cycle oscillations will not take place. This fact is shown in Fig. 18*b*, where it can be seen that the intersection between $G_{\text{ol}}(\text{j}\omega)$ and $-1/\mathcal{N}$ is avoided. The avoidance of the apparition of limit cycle oscillations has also been tested through a simulation with the same conditions as in the precedent case, which is presented in Fig. 19, where the system response to a unitary step change in the reference and disturbance input has been presented. As expected, this system does not present limit cycle oscillations, which shows that, effectively, a reduction on the ratio h/δ of the sampler lowers the robustness requirements of the system to avoid limit cycle oscillations.

Example 4: In an industrial environment, errors in the process model can appear due to several common causes, such as noisy measurement, few data for identification or non-linear behaviours, among others. The robustness margins serves to cope with the modelling error as well as with possible variations in the plant dynamic. Studying these margins for the worst-case scenario can be insightful to determine the actual robustness taking into account the uncertainty in the plant parameters. Furthermore, it is also possible to express the margins in terms of admissible variation in the parameters of the model, even though this analysis is valid only for the model structure that is being studied. This example illustrates these ideas.

Consider a process with nominal model given by the following transfer function:

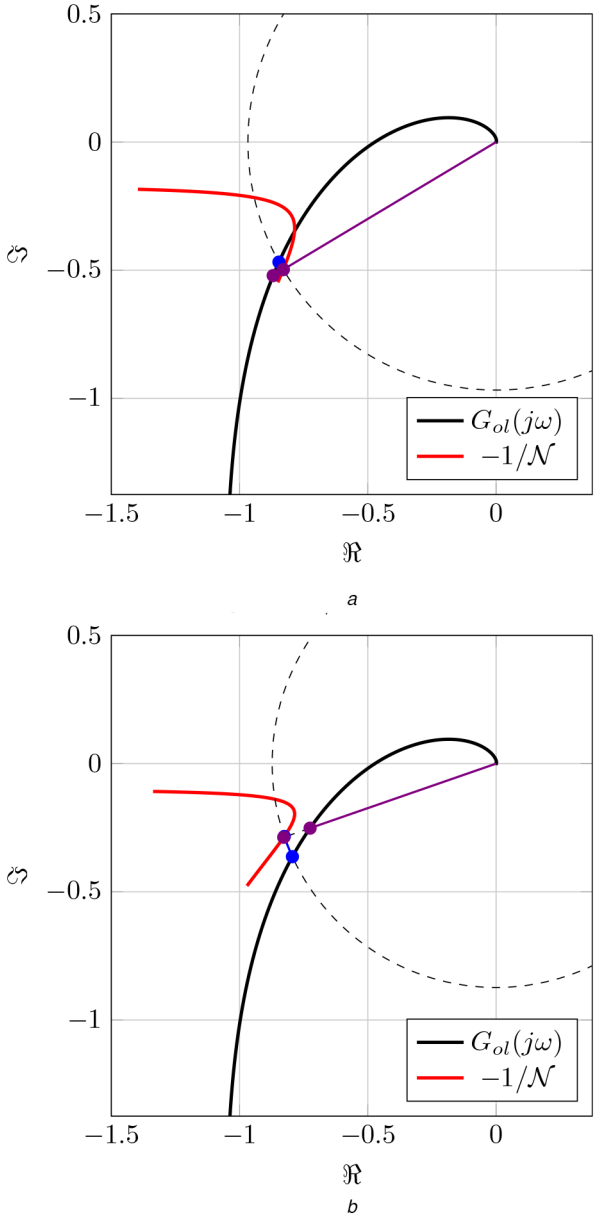

Fig. 18 *Nyquist diagram of G_{ol} with the inverse negative of the DF of its respective sampler*
(a) RQH with $h/\delta = 0.4286$, ***(b)*** RQH with $h/\delta = 0.25$

$$G(s) = \frac{e^{-0.2s}}{(s+1)^4} \tag{21}$$

whose gain, delay and poles have been obtained with a reliability of ±5%. A PI controller has been tuned using AMIGO tuning rules, obtaining $K_p = 0.281$ and $T_i = 2.41$. A RQH sampling with ratio $h/\delta = 1/3$ has been applied.

Due to the model uncertainties, the worst and best case scenarios, from the robustness point of view, are, respectively,

$$G_w(s) = \frac{1.05e^{-0.21s}}{(s+0.95)^4} \text{ and } G_b(s) = \frac{0.95e^{-0.19s}}{(s+1.05)^4}. \tag{22}$$

These models have been evaluated with the controller. The Nichols diagrams are depicted in Fig. 20, where it can be seen that the margins to the non-linearity vary from $\gamma_{h/\delta}$ =9.7 dB and $\Phi_{h/\delta}$ = 42.8° for the worst case to $\gamma_{h/\delta}$ =14.8 dB and $\Phi_{h/\delta} = 52°$ for the best case, being $\gamma_{h/\delta}$ =12.3 dB and $\Phi_{h/\delta}$ =48.3° the values obtained for the nominal model. In this case, the achieved margins are good enough to consider the system robust against oscillations induced by the sampler, even considering the effect of the model uncertainties.

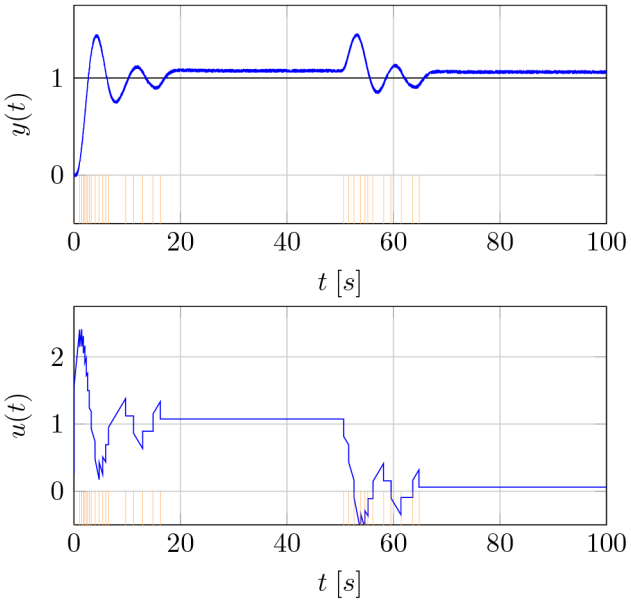

Fig. 19 *Controlled output y and control action u of a system with a RQH sampler with $h/\delta = 0.25$ in the loop, which avoids limit cycle oscillations*

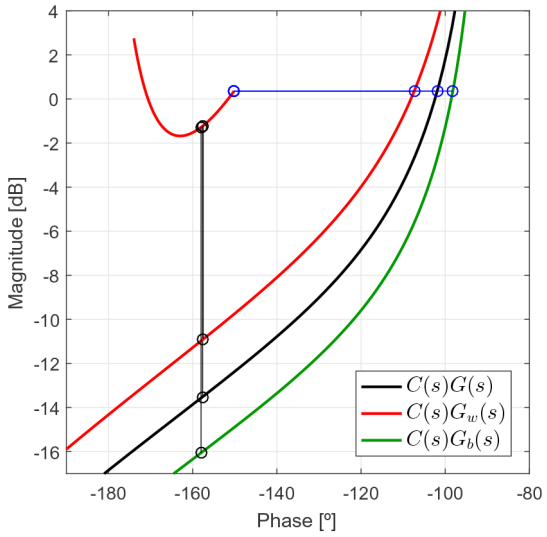

Fig. 20 *Robustness margins to the non-linearity for the modelled system and its best and worst-case scenarios due to uncertainty*

In addition to the previous study, the admissible variation of each nominal parameter without provoking limit cycle oscillation can be calculated. For this specific case, the gain can be increased until 4.11, the delay until 6.98 s and the multiple poles can be decreased to 0.75.

This kind of analysis allows expressing the robustness in terms of parameter variation, however, the results depend on the structure of $G_p(s)$.

7 Conclusions

In this paper, an alternative to either RQ or SSOD sampling strategies for event-based PI control systems has been presented. The proposed solution consists in an intermediate case between both strategies, attained by regulating the ratio between the quantification step and the quantifier hysteresis.

This solution presents several advantages regarding to RQ and SSOD. Firstly, it avoids sending events, and its associated data, through the network generated by changes in the sampled signal due to noise. In addition, it reduces the number of events needed to perform the control while still being reactive to significant changes in the state of the system.

To evaluate the robustness against limit cycles of the proposed sampling strategy the DF technique has been used, obtaining the regions that induce limit cycle oscillations on the system. From the knowledge of these regions, gain and phase margins to limit cycles induced by the RQH sampler have been defined.

Using these margins, the suitability of classical tuning methods for continuous systems, such as Ziegler–Nichols, Cohen–Coon, and AMIGO, can be evaluated when used for tuning controllers under RQH sampling strategy. An extensive simulation study shows that, even with good classical gain and phase margins provided by these methods, limit cycle oscillations can still be induced by the sampler if the proposed margins are negative.

The influence of the controller's parameters, network delay and model uncertainty on the proposed margins has been studied. The results reveal that the effect of varying these parameters on the new margins is similar to that obtained on classical gain and phase margins.

Additionally, the guidelines to select proper sampler parameters from noise and steady-state error specifications have been provided, and its influence in the limit cycle oscillations apparition and in the event generation has been addressed and highlighted through several examples.

8 Acknowledgments

This work was supported by MICINN project no. TEC2015-69155-R from the Spanish government, research project 18I411-Uji-b2018-39 from Universitat Jaume I and by CEICE grant no. ACIF/2018/244.

9 References

[1] Lunze, J.: 'Event-based control: introduction and survey', in Miskowicz, M. (Eds.): '*Event-based control and signal processing*' (CRC Press, Boca Raton, 2015), pp. 3–20

[2] Dotoli, M., Fay, A., Miśkowicz, M., *et al.*: 'An overview of current technologies and emerging trends in factory automation', *Int. J. Prod. Res.*, 2019, **57**, (15-16), pp. 5047–5067

[3] Aranda-Escolástico, E., Guinaldo, M., Heradio, R., *et al.*: 'Event-based control: a bibliometric analysis of twenty years of research', *IEEE Access*, 2020, **8**, (March), pp. 47188–47208

[4] O'Dwyer, A.: '*Handbook of PI and PID controller tuning rules*' (Imperial College Press, UK, 2006, 2nd edn.)

[5] Samad, T.: 'A survey on industry impact and challenges thereof', *IEEE Control Syst.*, 2017, **37**, (1), pp. 17–18

[6] Maxim, A., Copot, D., Copot, C., *et al.*: 'The 5w's for control as part of industry 4.0: why, what, where, who, and when a PID and MPC control perspective', *Inventions*, 2019, **4**, (1), pp. 1–10

[7] Årzén, K.-E.: 'A simple event-based PID controller'. Proc. 14th World Congress of IFAC, Beijing, March 1999, vol. Q, pp. 423–428

[8] Durand, S., Marchand, N.: 'An event-based PID controller with low computational cost'. 8th Int. Conf. on Sampling Theory and Applications (SampTA'09), Marseille, France, 2009

[9] Durand, S., Marchand, N.: 'Further results on event-based PID controller'. Proc. of the European Control Conf. 2009, Budapest, Hongrie, August 2009, pp. 1979–1984

[10] Vasyutynskyy, V., Kabitzsch, K.: 'A comparative study of PID control algorithms adapted to send-on-delta sampling'. Int. Symp. on Industrial Electronics (ISIE) 2010, Bari, Italy, July 2010, pp. 3373–3379

[11] Vasyutynskyy, V., Kabitzsch, K.: 'Time constraints in PID controls with send-on-delta', in Juanole, G., *et al.*, (Eds.): '*Fieldbuses and networks in industrial and embedded systems*, vol. 8, (Elsevier, USA, 2009), pp. 48–55

[12] Hsia, T.C.: 'Analytic design of adaptive sampling control law in sampled-data systems', *IEEE Trans. Autom. Control*, 1974, **19**, (1), pp. 39–42

[13] Dormido, S., Sánchez, J., Kofman, E.: 'Muestreo, control y comunicación basados en eventos', *Rev. Iberoamericana Autom. Inf. Ind. RIAI*, 2008, **5**, (1), pp. 5–26

[14] Ploennigs, J., Vasyutynskyy, V., Kabitzsch, K.: 'Comparative study of energy-efficient sampling approaches for wireless control networks', *IEEE Trans. Ind. Inf.*, 2010, **6**, (3), pp. 416–424

[15] Beschi, M., Dormido, S., Sánchez, J., *et al.*: 'Characterization of symmetric send-on-delta PI controllers', *J. Process Control*, 2012, **22**, (10), pp. 1930–1945

[16] Beschi, M., Dormido, S., Sánchez, J., *et al.*: 'Tuning of symmetric send-on-delta proportional-integral controllers', *IET Control Theory Appl.*, 2014, **8**, (4), pp. 248–259

[17] Pawlowski, A., Beschi, M., Guzmán, J.L., *et al.*: 'Application of SSOD-PI and PI-SSOD event-based controllers to greenhouse climatic control', *ISA Trans.*, 2016, **65**, pp. 525–536

[18] Romero, J.A., Sanchis, R., Peñarrocha, I.: 'A simple rule for tuning event-based PID controllers with symmetric send-on-delta sampling strategy'. Proc. of the 2014 IEEE Emerging Technology and Factory Automation (ETFA), Barcelona, Spain, September 2014, pp. 1–8

[19] Romero Pérez, J.A., Sanchis Llopis, R.: 'A new method for tuning PI controllers with symmetric send-on-delta sampling strategy', *ISA Trans.*, 2016, **64**, pp. 161–173

[20] Ruiz, Á., Beschi, M., Visioli, A., *et al.*: 'A unified event-based control approach for FOPTD and IPTD processes based on the filtered Smith predictor', *J. Franklin Inst.*, 2017, **354**, (2), pp. 1239–1264
[21] Sánchez, J., Guinaldo, M., Visioli, A., *et al.*: 'Identification of process transfer function parameters in event-based PI control loops', *ISA Trans.*, 2018, **75**, pp. 157–171
[22] Miguel-Escrig, O., Romero-Pérez, J.-A., Sanchis-Llopis, R.: 'Tuning PID controllers with symmetric send-on-delta sampling strategy', *J. Franklin Inst.*, 2020, **357**, pp. 832–862
[23] Miguel-Escrig, O., Romero-Pérez, J.-A., Sanchis-Llopis, R.: 'New robustness measure for a kind of event-based PID', *IFAC-PapersOnLine*, 2018, **51**, (4), pp. 781–786
[24] Romero Pérez, J.A., Sanchis Llopis, R.: 'Tuning and robustness analysis of event-based PID controllers under different event-generation strategies', *Int. J. Control*, 2017, **91**, pp. 1–21
[25] Åström, K.J., Hägglund, T., Astrom, K.J.: 'Advanced PID control', volume 461. ISA-The Instrumentation, Systems, and Automation Society Research Triangle, 2006
[26] Sun, L., Li, D., Lee, K.Y.: 'Optimal disturbance rejection for PI controller with constraints on relative delay margin', *ISA Trans.*, 2016, **63**, pp. 103–111
[27] Ziegler, J.G., Nichols, N.B.: 'Optimum settings for automatic controllers', *Trans. ASME*, 1942, **64**, (11), pp. 759–765
[28] Cohen, G.H., Coon, G.A.: 'Theoretical consideration of retarded control', *Trans. ASME*, 1953, **75**, (75), pp. 827–834
[29] Åström, K.J., Hägglund, T.: 'Revisiting the Ziegler-Nichols step response method for PID control', *J. Process Control*, 2004, **14**, (6), pp. 635–650
[30] Slotine, J.-J.E., Li, W.: '*Appied nonlinear control*' (Prentice Hall, USA, 1991)

10 Appendix

The output equation of the proposed sampler, whose input–output relation is presented in Fig. 3 is

$$\bar{e}(t) = \begin{cases} (i+1)\delta \ \text{ if } \ e(t) \geq (i+\frac{1}{2}+\frac{h}{2\delta})\delta \text{ and } \bar{e}(t^-) = i\delta, \\ \qquad\qquad i \in \mathbb{Z} \\ (i-1)\delta \ \text{ if } \ e(t) \leq (i-\frac{1}{2}-\frac{h}{2\delta})\delta \text{ and } \bar{e}(t^-) = i\delta \\ i\delta \qquad \text{if } \ e(t) \in [(i-\frac{1}{2}-\frac{h}{2\delta})\delta, (i+\frac{1}{2}+\frac{h}{2\delta})\delta] \\ \qquad\qquad \text{and } \bar{e}(t^-) = i\delta \end{cases} \tag{23}$$

For a sinusoidal input $e(\phi) = A\sin(\phi)$, the output of the sampler can be expressed as

$$\begin{aligned} \bar{e}(\phi) &= \delta \sum_{k=1}^{i} \operatorname{sgn}\left(\frac{\mathrm{d}e(\phi)}{\mathrm{d}\phi}\Big|_{\phi_k}\right) \quad \forall\phi; \phi_i < \phi < \phi_{i+1} \\ &= \delta \sum_{k=1}^{i} \operatorname{sgn}(\cos(\phi_k)) \end{aligned} \tag{24}$$

The EG-ZOH sampler is an odd non-linearity where the history of the input determines the value of the output in the multiple-valued regions. The DF for this kind of non-linearity is calculated as (see (25))

which can be rewritten as (see (26)) . Taking into account that

$$\int_{\phi_k}^{\pi} e^{-\mathrm{j}\phi}\mathrm{d}\phi = -\sin\phi_k - j(1+\cos\phi_k), \tag{27}$$

equation (26) results in

$$\begin{aligned} \mathcal{N}(A,h) = \frac{2\delta}{\pi A}\Bigg(&\sum_{k=1}^{n} (1+\cos\phi_k)\operatorname{sgn}(\cos\phi_k) \\ &-\mathrm{j}\sum_{k=1}^{n} \sin\phi_k \operatorname{sgn}(\cos\phi_k)\Bigg), \end{aligned} \tag{28}$$

which can be transformed to

$$\begin{aligned} \mathcal{N}(A,h) = \frac{2\delta}{\pi A}\Bigg(&\sum_{k=1}^{m} \cos\phi_k - \sum_{k=m+1}^{2m} \cos\phi_k \\ &-\mathrm{j}\left(\sum_{k=1}^{m} \sin\phi_k - \sum_{k=m+1}^{2m} \sin\phi_k\right)\Bigg). \end{aligned} \tag{29}$$

As the expressions of the $\sin\phi_k$ and $\cos\phi_k$ are known to be

$$\sin\phi_k = \begin{cases} \frac{\delta}{A}\left(k - \frac{1}{2} + \frac{h}{2\delta}\right) & \text{if } k = 1,2,\ldots,m \\ \frac{\delta}{A}\left(2m - k + \frac{1}{2} - \frac{h}{2\delta}\right) & \text{if } k = m+1, m+2, \ldots, 2m \end{cases} \tag{30}$$

$$\cos\phi_k = \begin{cases} +\sqrt{1-\left(\frac{\delta}{A}\left(k-\frac{1}{2}+\frac{h}{2\delta}\right)\right)^2} & \text{if } k = 1,2,\ldots,m \\ -\sqrt{1-\left(\frac{\delta}{A}\left(2m-k+\frac{1}{2}-\frac{h}{2\delta}\right)\right)^2} & \text{if } k = m+1, \\ & \qquad m+2,\ldots,2m \end{cases} \tag{31}$$

can be introduced in (29) which results in

$$\begin{aligned} \mathcal{N}(A,h) = \frac{2\delta}{A\pi}\Bigg[&\sum_{k=1}^{m} \sqrt{1-\left(\frac{\delta}{A}\left(k+\frac{h}{2\delta}-\frac{1}{2}\right)\right)^2} \\ &+\sum_{k=m+1}^{2m} \sqrt{1-\left(\frac{\delta}{A}\left(2m-k-\frac{h}{2\delta}+\frac{1}{2}\right)\right)^2}\Bigg] - \mathrm{j}\frac{2hm\delta}{A^2\pi} \end{aligned} \tag{32}$$

$$\begin{aligned} \mathcal{N}(A,h) &= \frac{2j}{\pi A}\int_0^{\pi} \bar{e}(\phi)e^{-\mathrm{j}\phi}\mathrm{d}\phi \\ &= \frac{2j}{\pi A}\Bigg(\int_{\phi_1}^{\phi_2} \delta\operatorname{sgn}(\cos\phi_1)e^{-\mathrm{j}\phi}\mathrm{d}\phi + \int_{\phi_2}^{\phi_3} \delta(\operatorname{sgn}(\cos\phi_1) \\ &\quad +\operatorname{sgn}(\cos\phi_2))e^{-\mathrm{j}\phi}\mathrm{d}\phi + \cdots + \int_{\phi_n}^{\pi} \delta\sum_{k=1}^{n}(\operatorname{sgn}(\cos\phi_k))e^{-\mathrm{j}\phi}\mathrm{d}\phi\Bigg) \end{aligned} \tag{25}$$

$$\begin{aligned} \mathcal{N}(A,h) &= \frac{2\delta j}{\pi A}\Bigg(\int_{\phi_1}^{\pi} \operatorname{sgn}(\cos\phi_1)e^{-\mathrm{j}\phi}\mathrm{d}\phi + \int_{\phi_2}^{\pi} \operatorname{sgn}(\cos\phi_2)e^{-\mathrm{j}\phi}\mathrm{d}\phi \\ &\quad +\cdots + \int_{\phi_n}^{\pi} \operatorname{sgn}(\cos\phi_n)e^{-\mathrm{j}\phi}\mathrm{d}\phi\Bigg) \\ &= \frac{2\delta j}{\pi A}\sum_{k=1}^{n}\left(\operatorname{sgn}(\cos\phi_k)\int_{\phi_k}^{\pi} e^{-\mathrm{j}\phi}\mathrm{d}\phi\right). \end{aligned} \tag{26}$$